Advances in running ductile fracture assessment for the Longship full-scale CCS project

Gaute Gruben[1] and Kenneth Macdonald[2]

[1] SINTEF Industry, Trondheim, Norway
[2] Equinor ASA, Stavanger, Norway

ABSTRACT: As an integral part of the Norwegian full-scale CCS project Longship, the Northern Lights joint venture owned by Equinor, Shell and Total, is responsible for transporting liquified CO2 by ship from the industrial capture sites in the south-eastern part of Norway to an onshore terminal located on the Norwegian west coast. From the terminal, the liquified CO_2 will be transported by a 12 ¾'' OD offshore pipeline to the Johansen reservoir in the North Sea for permanent storage. Fracture control of the pipeline is essential for safe and robust CO_2 transportation during the whole operational lifetime. The presently available international guidance for CO_2 transport (in the form of Standards and Recommended Practices) rests with ISO 27913 and DNVGL-RP-F104. This involves designing the pipeline such that a rupture, that might occur due to e.g. accidental loads, will arrest rather than evolve into a more extensive running ductile fracture. However, the multi-phase behavior of expanding liquified CO_2 induces a larger crack-driving force on a propagating crack compared to lean or rich natural gas. Several studies have shown that prediction of the crack arrest/propagation boundary is challenging under such conditions. In this study a previous concept-phase assessment of the Northern Lights pipeline is revisited, and a new evaluation is conducted based on some of the latest developments in analytical methodologies for design against running ductile fracture. The new evaluation is performed in combination with recent minor amendments to the design basis for the pipeline. The main conclusion from the present study is that the wall thickness of 15.9 mm remains sufficient for arresting a propagating crack.

1. INTRODUCTION

Figure 1 illustrates the chain of the planned full-scale Norwegian CCS project Longship. The Northern Lights CO_2 transport system is an integral part of this chain, where an onshore terminal will receive CO_2 transported by ship tankers from industrial source sites located in south-eastern Norway, temporarily store liquid CO_2 onshore in tanks at the terminal, and finally transport CO_2 via a 12 ¾'' OD offshore pipeline for injection into the Johansen storage reservoir in the North Sea. The CO_2 injection pipeline will be laid to a subsea structure where the fluid will be injected. The pipeline is sized for the transport volumes from the CO_2 capture sites under the existing contract with Gassnova, but with additional capacity to accommodate defined future volumes.

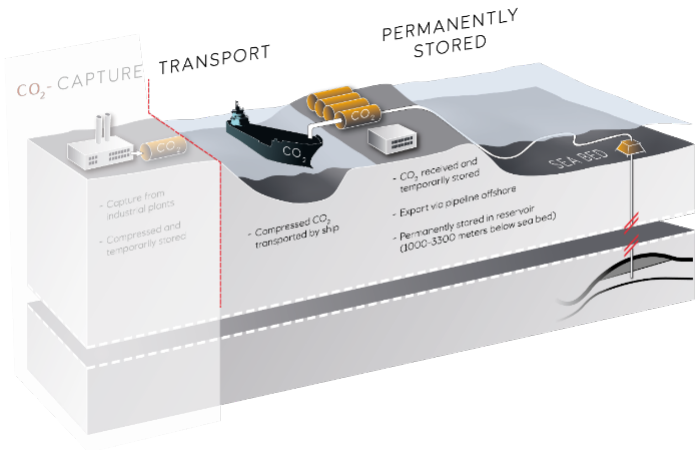

Figure 1. Concept of the Northern Lights transport and storage as part of the Longship full-scale CCS chain

Longitudinal running ductile fracture (RDF) is a catastrophic event that may occur in pressurized pipelines. An initial fracture caused by e.g., an accidental load, can lead to a rupture that can either be immediately arrested or evolve into a running ductile fracture. If the transported fluid has a high decompression speed, which typically is the case for liquid-phase fluids like water or oil and some gaseous-phase fluids like hydrogen, the pressure (or the crack-driving force) downstream the crack tip will rapidly drop, and the rupture will arrest (Cosham et al., 2012). However, if the fluid has a low or delayed decompression speed, which is the case for e.g. natural gas, the crack-driving force can push the fracture over long distances. Releasing the energy stored in the pressurized fluid results in an explosion that can have severe consequences for the surroundings, therefore it is essential to design the pipeline so that an eventual rupture does not evolve into RDF. Based on an extensive experimental dataset, researchers at the Battelle Memorial Institute in the 1960s and 70s developed a design equation, the Two Curve Method (TCM) (Maxey, 1974). Here, a semi-empirical curve with the crack velocity expressed as a function of pressure is compared with the decompression velocity curve of the fluid. The TCM gives a good indication of the arrest/propagation boundary for steel pipes with yield strength less than ~450 MPa and Charpy V-notch values (CVN) less than ~100 J. Most modern steel pipes have improved fracture toughness properties, CVN > 150 J, and the TCM have proven to not capture the arrest/propagate boundary for such steels. This has led to successful proposals for modification factors to the measured CVN value (Wilkowski et al., 1977, Leis et al., 1998) to enhance the reliability of the Two-Curve Method for steel pipes with high toughness. However, when this type of modification is applied to high-strength pipeline steels, the TCM equations are not able to predict the arrest/propagate boundary (Demofonti et al., 2005, Andrews et al., 2003, Papka et al., 2003). As for CO_2 pipelines with moderate yield strength, recent studies have shown that the TCM method with CVN modification gives non-conservative results for RDF design (Cosham, 2012, Cosham et al., 2014). The main reason stems from the physics of CO_2 during depressurization as compared to e.g. natural gas; when the liquid-phase CO_2 expands, a thermodynamic process leads to a phase-change and the CO_2 begins to boil creating a mixed liquid-phase and gaseous-phase fluid. The liquid-phase decompression speed of CO_2 is typically higher that the speed of a ductile fracture, and so the CO_2 between the crack-tip and the primary decompression wave has a two-phase state with a pressure equal to the CO_2 boiling pressure. This gives a higher pressure at and downstream the crack-tip (and thus a larger crack-driving force) than what typically is the case for natural gas. Maxey (1986) addressed the differences between natural gas pipelines and CO_2 pipelines with respect to RDF and proposed the TCM to be a two-point method rather than a two-curve method where the boiling pressure of the CO_2 must be lower than the 'arrest pressure' as defined by the pipeline to ensure crack arrest. This approach is mentioned in ISO/TC 265 (2016) where a safety factor on the calculated arrest pressure in cases where CVN<330 J is recommended. The available full-scale test data on CO_2 pipelines are scarce compared to natural gas pipelines. However, four projects have produced full-scale data over the last decade; CO2PIPETRANS (Aursand et al., 2016), COOLTRANS (Barnett and Cooper, 2014), SARCO2 (Di Biagio et al., 2017) and CO2SafeArrest (Linton et al., 2018). Based on data from these projects, Michal et al. (2020) proposed a modification of the TCM that is used as basis for the design approach in the most recent version of DNVGL-RP-F104 (2021).

As an alternative to analytical methods like the TCM, numerical methods have also been used for assessing RDF problems. In most studies the fluid is in gaseous phase e.g. (O'Donoghue et al., 1997, Shim et al., 2008, Nakai et al., 2016), but more recently numerical analyses with CO_2 have also been presented e.g. (Mahgerefteh et al., 2012, Aursand et al., 2016, Keim et al., 2020). The importance of including the backfill in RDF analysis has been pointed out by e.g. (Gruben et al., 2018a, Nonn et al., 2020). The Northern Lights pipeline is based on the Mongstad pipeline and so a requalification of this pipeline with respect to RDF was performed by SINTEF in 2018, see (Gruben et al., 2020) as part of the project's concept development phase. Since 2018, the design basis for the Northern Lights pipeline has been adjusted slightly and further developments in TCM analysis have been established, thus the pipeline is assessed here with the updated design basis and the revised analytical method.

2. DESIGN BASIS

In the front-end engineering phase, three alternative pipeline routes were considered, all leading to a pipeline with an approximate length of 70 km and with an onshore section of maximum 10 km (Gruben et al., 2018b). Since the transport of the CO_2 to the onshore terminal is by ship and in the liquid state, the CO_2 capture stream is considered (by specification) to be free of impurities capable of increasing the boiling pressure. The significance and effects of important impurities in the capture stream on gas decompression characteristics have been investigated experimentally, see e.g. Munkejord et al. 2021. These factors are directly addressed by the specification limits for the capture volumes at source. The industrial capture site and ship transport configuration of the Longship project's operating model precludes any temporary process upset scenarios that would otherwise be of concern for systems based on continuous stream-related capture and storage. Thus, the maximum possible loading pressure in an RDF event due to volume expansion of CO_2 equals the critical point of pure CO_2 which is 7.4 MPa. This is illustrated as load case V in Figure 2. However, pressure of such values is not likely to occur in the Northern Lights pipeline, and an analysis of different scenarios was conducted (Gruben et al., 2018b). Based on conservative assumptions, the highest calculated saturation pressure was estimated as 5.6 MPa, shown as load case I in Figure 2. In the front-end engineering phase, the design operation pressure was 250 bar and based on an assumed wellhead pressure of 75 bar, which is the minimum wellhead pressure to secure single-phase liquid in the pipeline. The design operation pressure has since been increased to 310 bar, but this will lower the saturation pressure in case of a pipe rupture. This is illustrated by load cases, II, III and IV in Figure 2, which shows the calculated saturation pressure after decompression for pure CO_2 with different initial pressures, but with the same initial temperature. Thus, assuming a low initial pressure of 57 bar in load case I is conservative with respect to the expected initial pressure which might be as high as 310 bar. Note that the wellhead pressure may also be higher depending on the reservoir pressure and the frictional pressure loss in the well.

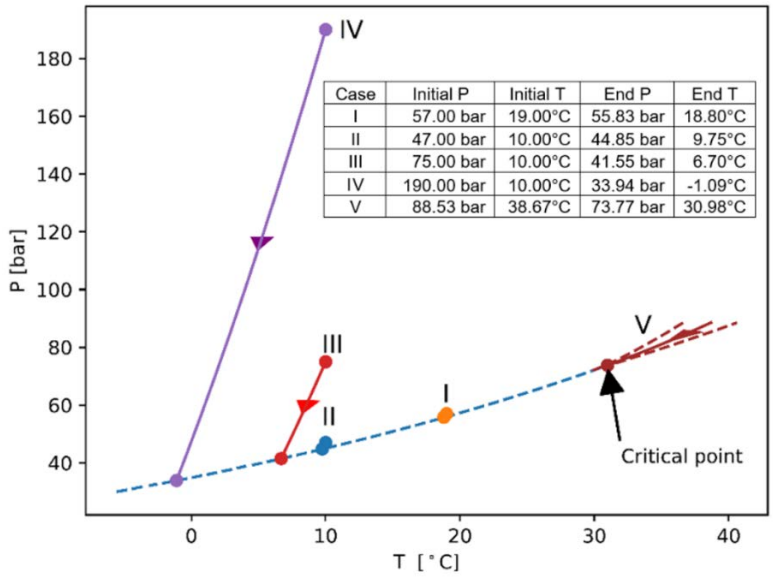

Case	Initial P	Initial T	End P	End T
I	57.00 bar	19.00°C	55.83 bar	18.80°C
II	47.00 bar	10.00°C	44.85 bar	9.75°C
III	75.00 bar	10.00°C	41.55 bar	6.70°C
IV	190.00 bar	10.00°C	33.94 bar	-1.09°C
V	88.53 bar	38.67°C	73.77 bar	30.98°C

Figure 2 The saturation pressure (blue dashed line) and 5 different load cases

The onshore and offshore pipeline sections have identical input parameters. The pipeline is of grade DNVGL 450 (X65) and the geometry is based in part on dominant design demands for reeled installation. Both seamless and HFW pipes were originally considered, as HFW line pipe potentially offered economic advantages. The given parameters relevant for the present study are summarized below.

- Nominal outer diameter, *D*: 323.9 mm
- Nominal wall thickness, *t*: 15.9 mm
- Specified minimum yield stress at 20 ºC: SMYS=450 MPa
- Specified minimum tensile strength at 20 ºC: SMTS=535 MPa
- Maximum yield to tensile ratio: 0.92
- Young's modulus, *E*: 207 GPa
- Poisson's ratio: 0.3
- Charpy V-notch (CVN) value: minimum specified 125 J, actual 200-450 J. Design is to be conducted for 100 J, 125 J and 200 J
- Drop Weight Tear Test (DWTT) requirement: 85 % shear area at minimum operating temperature

3. ANALYSIS WITH THE TWO-CURVE METHOD

3.1 General TCM analysis for natural gas and CO2 pipelines

When performing analysis with the two-curve method, the material's CVN energy required to arrest a running fracture for a fluid with a given initial state is sought. The original TCM is based on an equation expressing the materials critical hoop stress at the crack-tip, σ_a, for arresting a fracture expressed as (Maxey, 1974):

$$\frac{1000 \cdot CVN \cdot E}{A_c \sigma_f^2 \sqrt{Rt}} = \frac{24}{\pi} \ln\left(\sec\left(\frac{\pi}{2}\frac{3.33\sigma_a}{\sigma_f}\right)\right) \quad [1]$$

where R is the pipe radius, A_c is the area of the Charpy specimen, and σ_f is the equivalent flow stress of the pipe material. All units in Eq. 1 are given in mm, MPa and J. The core of Eq. 1 is the then contemporary strip-yield fracture model (Burdekin and Stone, 1966), which is modified to account for pipe geometry, material work hardening, crack-arrest instead of onset of crack propagation, and a relation between the stress intensity factor and the CVN value. In a design situation the hoop stress at the crack-tip must be evaluated and compared to the critical hoop stress given in Eq. 1. The pipe's arrest capacity in the static limit is commonly expressed by the arrest pressure, p_a, which is related to the critical hoop stress as $p_a = \sigma_a t/R$. By rearranging Eq. 1, the arrest pressure is expressed as a function of the pipe geometry and material properties as:

$$p_a = \frac{2\sigma_f \cdot t}{3.33\pi R} \arccos\left(\exp\left(-\frac{1000 \cdot CVN \cdot E\pi}{24 A_c \sigma_f^2 \sqrt{Rt}}\right)\right) \quad [2]$$

Based on the assumption that the local sonic speed of a single-phase gas at the open end equals the local particle velocity relative to the moving fracture, the original TCM estimated the pressure at the crack tip by the following equation (Maxey et al., 1972)

$$p(V) = p_L\left(\frac{2}{\gamma+1} + \frac{\gamma-1}{\gamma+1} \cdot \frac{V}{C_L}\right)^{\frac{2\gamma}{\gamma-1}} \quad [3]$$

where V is the crack velocity, C_L is the acoustic velocity at the initial operating pressure, p_L, and γ is the ratio of the specific heat at constant pressure to the specific heat at constant volume. From Eq. 1, the limit of zero crack velocity has a pressure equal to $p_0 = p_L(2/(\gamma+1))^{2\gamma/(\gamma-1)}$, while the pressure at the instant of a rupture in the pipe is near the operating pressure, p_L. Due to the relatively high pressure at onset of a rupture, the crack will experience a high crack-driving force with a corresponding high initial velocity before it enters either a steady-state velocity with a pressure between p_0 and p_L, or it arrests. The high initial velocity can be referred to as the 'opening effect'. Experimental data from full-scale burst tests showed that the pressure at the crack-tip in an RDF was higher than the critical pressure at the crack-tip in the static limit as expressed by Eq. 1. Based on an expression of the plastic wave speed in the steel material and data from full-scale burst tests, an empirical relation between the pressure at the crack-tip and the crack velocity was established as

$$p_a^{dyn}(V) = p_a\left[\left(V\frac{\sqrt{CVN/A_c}}{K_{BF}\cdot\sigma_f}\right)^6 + 1\right] \quad [4]$$

where K_{BF} is a backfill coefficient and p_a is the arrest pressure in the static limit as defined in Eq. 2. Now with the expression of the pressure at the crack-tip (Eq. 3) and the expression of the critical pressure at the crack-tip of the RDF (Eq. 4), the criterion for arresting an RDF can be expressed as $p(V) < p_a^{dyn}(V)$ for all V, this is illustrated by *Fracture curve 1* in Figure 3(a) below. This can be interpreted as a case where the decompression wave outruns the propagating crack. In the case of a predicted steady-state fracture, the two curves intersect at least once, and the resulting fracture velocity is defined as the highest intersection velocity. This is illustrated by *Fracture curve 2* in Figure 3(a), which predicts a steady-state fracture velocity of ~100 m/s.

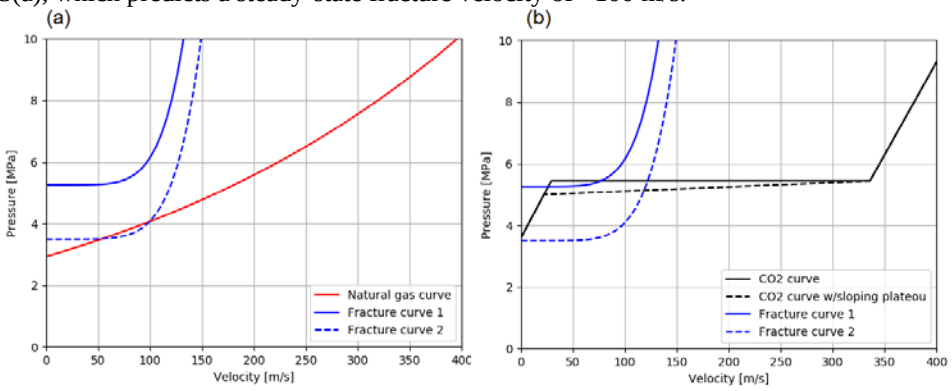

Figure 3 (a) TCM with natural gas loading and predicted arrest (Fracture curve 1) and with predicted propagation (Fracture curve 2). (b) Illustrates the same fracture curves together with CO_2 loading curves with and without sloping plateau. Fracture curve 2 gives propagation for both CO_2 loading curves, while Fracture curve 1 gives arrest for the CO_2 curve with sloping plateau.

In the case of a rupture in a pipeline transporting dense-phase CO_2, a completely different process occurs in the fluid during decompression. The CO_2 will undergo a phase-change from a liquid state to a two-phase state of boiling fluid. This implies that the pressure upstream the crack-tip is near constant in a CO_2 pipeline, while in a gas pipeline, a steady decrease is present between the operation pressure and the pressure at the crack-tip, this is illustrated in Figure 4. The boiling pressure for pure CO_2 can be estimated as the saturation pressure by e.g. the Span-Wagner model (Span and Wagner, 1996). In a traditional TCM plot, the phase-change results in a sudden drop in wave velocity at a given pressure as illustrated by the solid line CO_2 curve in Figure 3(b). If we consider this CO_2 curve as our loading case, both *Fracture curve 1* and *2* will lead to a steady-state propagating crack, but with fracture velocities at ~75 m/s and ~125 m/s respectively. One important point illustrated in Figure 3(b) and in Figure 4, is that the plateau stemming from the boiling CO_2 likely gives a higher loading pressure at the crack-tip than in the case of natural gas for the range of most relevant crack velocities (<200 m/s). Another important point illustrated in Figure 3(b) is that the second drop in CO_2 pressure occurs at such low wave velocity that the benefit of the increased crack resistance in the propagating crack will not influence the predicted arrest/propagation boundary. Thus, the saturation pressure (p_s) and the arrest pressure in the static limit (p_a) are sufficient information to predict arrest/propagate for a given pipeline. This was pointed out in (Maxey, 1986). The criterion for arresting a crack in a CO2 pipeline is then expressed as:

$$p_s \leq p_a \quad [4]$$

However, from full-scale burst tests it is found that the actual pressure at the crack-tip is ~0.8 MPa lower than the calculated saturation pressure (Michal et al., 2020). This effect is illustrated as a sloping pressure plateau in Figure 3(b). The exact reason for this effect is still a research question. If the sloping plateau is considered, *Fracture curve 2* will lead to arrest for this load case. However, as a conservative measure, the saturation pressure should be used as a basis in a design situation. On the other hand, if a criterion for predicting the arrest/propagate boundary is to be established from full-scale testing, the sloping plateau must be included. Studies from full-scale testing on CO_2 have shown that using Eq. 4 without safety factors gives unconservative results, e.g. (Cosham et al., 2016, Di

Biagio et al., 2017). In ISO 27913 (2016) Annex D, a TCM analysis with a safety factor of $c_{cf} \geq 1.2$ is recommended, thus the design criterion can be expressed as

$$p_s \leq p_a / c_{cf} \quad [5]$$

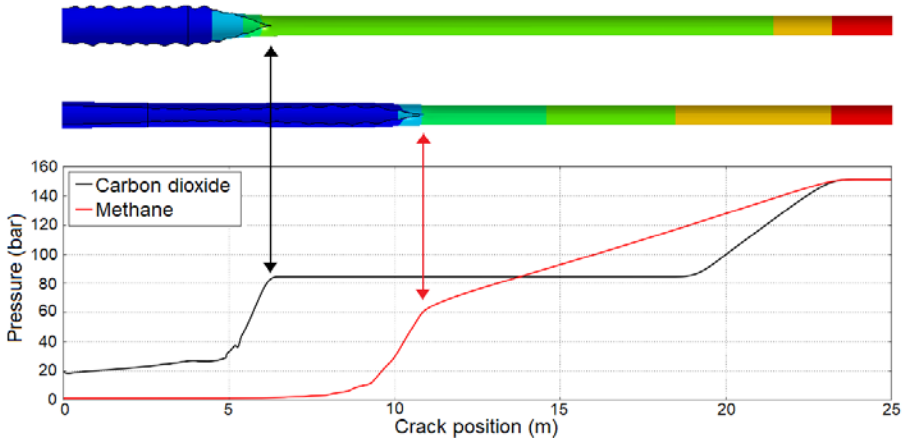

Figure 4 Illustration of pressure drop upstream and downstream the crack-tip in natural gas and CO_2 pipeline.

The present state-of-the art for TCM analysis of CO_2 pipelines was given by Michal et al. (2020) which presented a novel criterion for predicting the arrest/propagation boundary based on the results from 8 full-scale burst tests carried out in four different projects. Since the crack velocity is not an important parameter in such analysis due to the low velocity at the second pressure drop, the criterion was established from the measured pressure in each pipe segment and the relevant geometrical and mechanical properties of each pipe section. That is, the sloping pressure plateau illustrated in Figure 3(c) was accounted for. The data was divided in two sets with 'propagate' and 'arrest' and plotted in the space of Eq. 1, i.e. the abscissa values represented the pipe properties as expressed by the left-hand side of Eq. 1 and the ordinate represented the ratio of the measured hoop stress and the pipe sections yield stress. By separating the data with propagating cracks from data with crack arrest, it was possible to define an empirical criterion that distinguished the parts of expected arrest from the parts with expected propagation. The resulting criterion has been implemented in the most recent version of DNVGL-RP-F104 (2021) where three regions have been identified marked in Figure 5(a) as, 'Propagation expected', 'Arrest expected' and 'Special assessment needed'. The reason for defining a region with need of special assessment is due to the lack of data from full-scale tests for abscissa values < 25. Michal et al. (2020) proposed that a straight line from origin to the point (25, 0.23) in Figure 5(a) could be a reasonable criterion for low abscissa values, this is illustrated in Figure 5(b). However, they did not firmly conclude on this due to the lack of experimental data in this region. When published, the revised DNVGL- RP-F104 (2021) omitted this proposal, opting instead for a vertical line from the same point (25, 0.23). DNVGL- RP-F104 (2021) also summarizes the following six limitations for design based on TCM:

1. Pipeline steel grades must be X60-X65
2. Applicable for submerged arc-welded TMCP pipes[1]
3. Pipeline content is overwhelmingly CO_2
4. Pipeline diameter is between 16" and 26"
5. Wall thickness is between 10 mm and 26 mm
6. The Charpy test must have similar fracture mechanisms as the ones observed in the full-scale tests used for development of the model[2]

[1] HFW pipes are currently not considered to be covered by criteria due to the possibility of the pipes having high Y/T ratios at some circumferential locations

[2] This is likely being fulfilled if the CVN energy is 250 J or higher

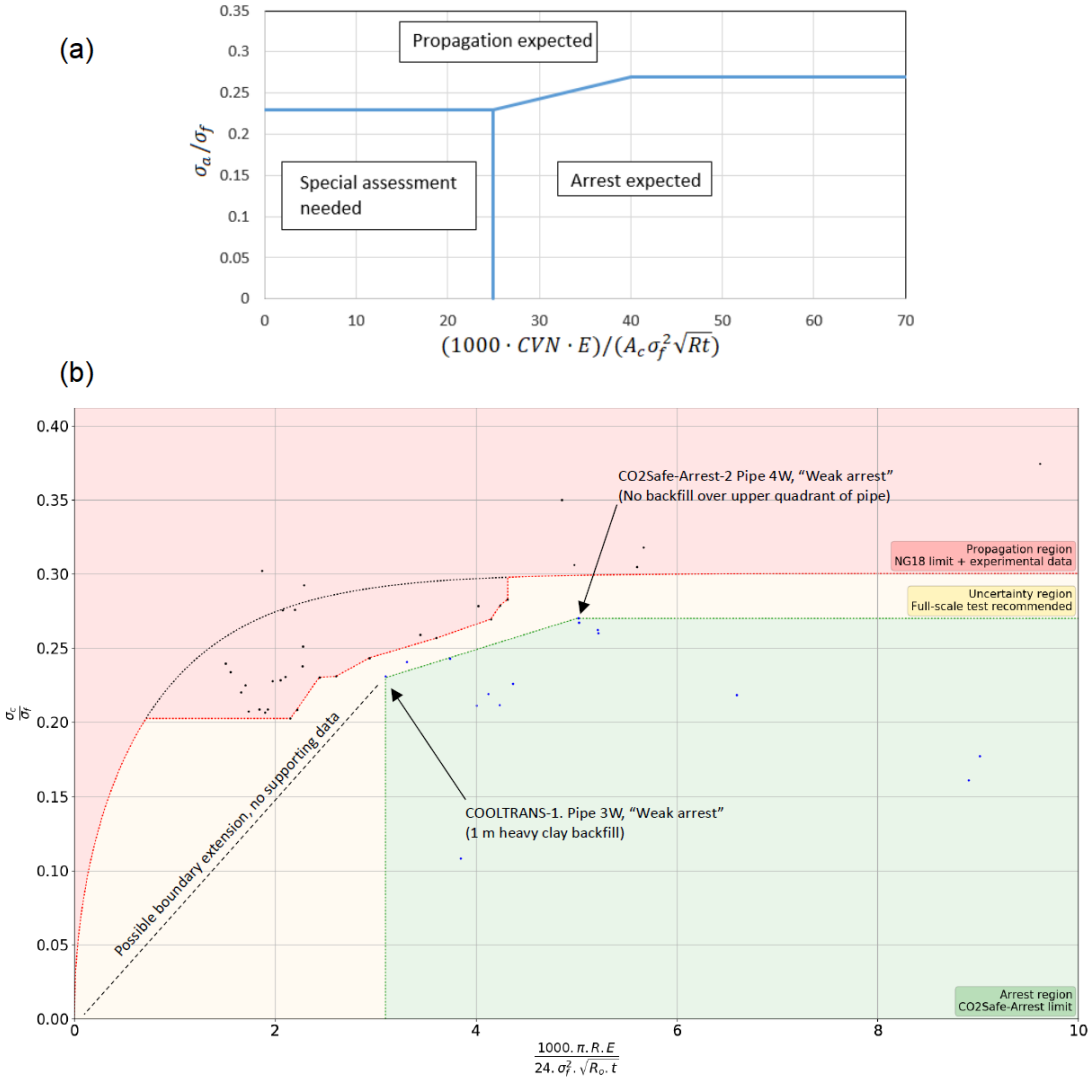

Figure 5 (a) Three regions of predicted outcome from TCM in DNVGL-RP-F104 (2021). (b) Experimental data and three regions of propagation, uncertainty and arrest from Michal et al. (2020)

3.2 TCM analysis for the Northern Lights pipeline

In Gruben et al. (2018a) the Northern Lights pipeline was assessed with the TCM analysis based on the recommendations in the then applicable DNV-GL RP-F104 (2017). Here, to avoid unstable crack propagation the following condition must be fulfilled:

$$p_s \cdot \gamma_{sat} \leq p_a/\gamma_{CO2} \quad [6]$$

where γ_{sat} is a loading coefficient and γ_{CO2} is a material coefficient. As can be observed, Eq. 6 has the same shape as the design equation from ISO 27913 (Eq. 5). DNV-GL RP-F104 (2017) did not specify values for γ_{sat} and γ_{CO2}, but as a conservative measure, Gruben et al. (2018a) applied $\gamma_{sat} = 1.3$ which gave an effective loading pressure close to the critical limit of pure CO_2 ($1.3 \cdot 5.5$ MPa $= 7.1$ MPa), see also Figure 2. This value will also be applied in the following example. The material coefficient was set as $\gamma_{CO2} = 1.2$ as recommended in ISO 27913 and will also be used in the following example.

By applying the design basis for the Northern Lights pipeline from Section 2 and defining $\sigma_f = SMYS + 69$ MPa $= 519$ MPa and $A_C = 80$ mm^2, Eq. 2 gives the resulting arrest pressure for the design CVN values of 100 J, 125 J and 200 J as 14.5 MPa, 14.8 MPa and 15.2 MPa, respectively. Considering $\gamma_{CO2} = 1.2$, the CVN=100 J case gives $p_a/\gamma_{CO2} = 12.1$ MPa, i.e. 70 % higher than $p_s \cdot \gamma_{sat} = 7.1$ MPa. In other words, even for the case of a very low CVN value of 100 J, the Northern Lights pipeline will have abundant capacity to arrest a

RDF following DNVGL-RP-F104 (2017). Another observation is that the arrest pressure is nearly saturated with respect to the CVN value, thus the pipe is in the 'stress-controlled' region.

The question now is how a fresh assessment with the updated DNVGL-RP-F104 (2021) will turn out. First, the loading pressure is defined from a conservative estimate of the highest saturation pressure, i.e. a pressure differential of 5.5 MPa as calculated in load case I in Section 2. It is noted that the calculation of this loading pressure is conservative with respect to initial temperature and line pressure. The resulting hoop stress is then $\sigma_h = p \cdot R/t = 112$ MPa, and the normalized hoop stress is $\sigma_h/\sigma_f = 0.11$. The abscissa value depends on CVN and is then, $X = (1000 \cdot CVN \cdot E)/(A_c\sigma_f^2\sqrt{Rt})$=18.9, 23.7 and 37.9 for CVN of 100 J, 125 J and 200 J, respectively. As can be seen from Figure 6, CVN values of 100 J and 125 J place results in the 'Special assessment' region, while the CVN=200 J case is positioned in the 'Arrest expected' region. Interestingly and counter-intuatively, if we halve the wall thickness of the pipe to 7.95 mm all three CVN cases reside in the 'Arrest expected' region. Since the fracture resistance of a *t*=15.9 mm pipe obviously is significantly larger than for a *t*=7.95 mm pipe, we can safely assume a rapid crack arrest given the other five limitations in DNVGL-RP-F104 (2021), are fulfilled.

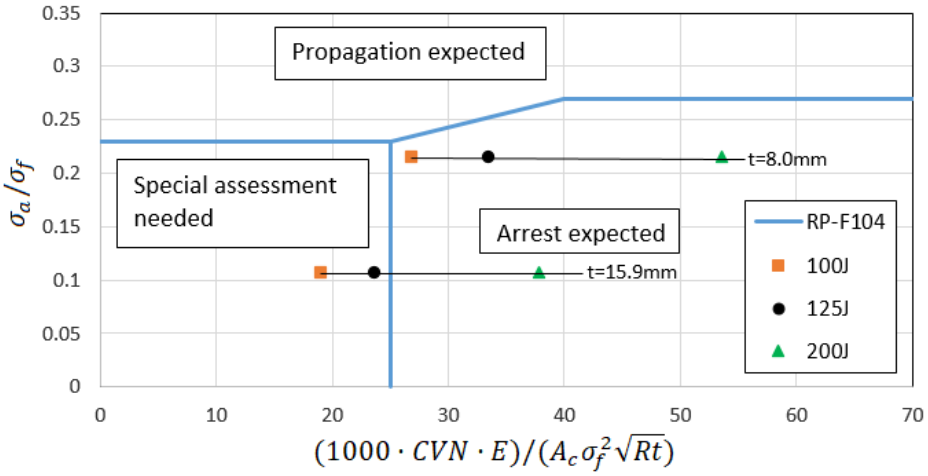

Figure 6 The Northern Lights pipeline assessed for three CVN values and for planned 15.9 mm wall thickness and for reduced wall thickness of 8.0 mm.

Regarding the additional limitations in the revised DNVGL-RP-F104 (2021), the following observations are made relating to the Northern Lights pipeline:

1. The Northern Lights pipeline has the same strength as the X60/X65 pipe segments applied for establishing the criteria in Figure 6
2. The design basis states explicitly a low yield to tensile strength ratio (<0.92) irrespective of linepipe type.
3. Pipeline content is assumed to be pure CO_2 since it is transported in liquid phase to the terminal
4. The diameter in the Northern Lights pipeline is a factor 0.8 lower than the smallest diameter in the pipe segments applied in the empirical data-set for establishing the criterion in Figure 6. Reducing the diameter implies reducing the crack-driving force since the pressure downstream the crack-tip works on a smaller area, while the pipe segment's resistance against a propagating fracture relies on the material properties and the wall thickness. Thus, the reduced thickness of the Northern Lights pipeline compared to the segments in the empirical dataset is not considered critical in the TCM design.
5. The Northern Lights pipeline has a wall thickness in the range of the tested pipe segments.
6. The Charpy test samples must be investigated to make sure the fracture mechanism is the same as the one in an expected RDF. In the experimental dataset for deriving the fracture criterion, two segments from the CO2PIPETRANS project with CVN=121 J and 144 J experienced arrest, thus a strict criterion on CVN values above 250 J does not seem necessary.

4. DISCUSSION

Gruben et al. (2020) estimated the minimum wall thickness from TCM and computational mechanics simulations. Here, based on several conservative assumptions, a minimum wall thickness of ~10 mm was predicted for both the TCM and the numerical analyses, although the numerical simulations predicted a dependency on the CVN value giving a minimum wall thickness ranging between ~10.0 mm and ~11.5 mm for CVN values between 100 J and 200J. In the following, the minimum wall thickness based on load case I from Section 2 (differential pressure equal to 54.8 MPa) following TCM analysis with is shown. The criteria for establishing the minimum wall thickness are the original TCM equation (Eq. 1), the ISO 27913 criterion with $c_{cf} = 1.2$ (Eq. 5) and the DNVGL-RP-F104 (2021) criterion with the modification of a straight line between the origin and the point (25, 0.23) as suggested as a possible limit by Michal et al. (2020). All three criteria are plotted in the same space in Figure 7(a), and the minimum wall thickness for the Northern Lights pipeline based on each criterion and CVN value are shown. First one can observe that the original TCM limit is the least conservative criterion for all abscissa values and positioned a factor 1.2 above the ISO 27913 limit. Further, the RP-F104 criterion with the proposed modification is the most conservative criterion for abscissa values less than ~30, while this criterion is positioned between the other two criteria for abscissa values above ~30. Another observation is that the TCM and the ISO27913 at an abscissa value of 25 is 2.5 % from the saturation value, while the DNVGL-RP-F104 criterion is 17 % from the saturation value. Now, as can be seen from Figure 7(a), the abscissa value of the pipe is strongly dependent on the CVN value, but for the TCM and the ISO27913 criteria the minimum wall thickness remains practically the same for the applied range of CVN since these two criteria are saturated. The TCM predicts a minimum wall thickness of ~5.7 mm, while the more conservative ISO27913 criterion predicts a minimum wall thickness of ~6.9 mm. Following the RP-F104 criterion, the wall thickness for CVN=100 J is 7.2 mm and reduced by 10 % to 6.5 mm for CVN=125 J, and by 12.5 % to 6.3 mm for CVN=200 J. It is clear that the DNVGL-RP-F104 criterion introduces an increased sensitivity for the CVN value in the Northern Lights pipeline, in the same manner as was observed in computational mechanics analyses in (Gruben et al., 2020).

When the loading pressure is increased, the minimum wall thickness is increased, and so the abscissa position of the pipe is shifted leftwards. This is illustrated in Figure 7(b) where the load pressure is 7.28 MPa. In response to this, the TCM and the ISO27913 criteria are somewhat more sensitive to the CVN value, but still the difference in predicted minimum wall thickness for CVN=100 J and CVN=200 J is less than 2.5 %. As for the DNVGL-RP-F104 criterion, the CVN=100 J case is here limited by the line denoted Michal et al. in Figure 7(b), and due to the high gradient of this line, the sensitivity to the CVN value is increased. This is reflected in the minimum wall thicknesses which are reduced by 16 % and 21 % for the CVN=125 J and the CVN=200 J cases, respectively.

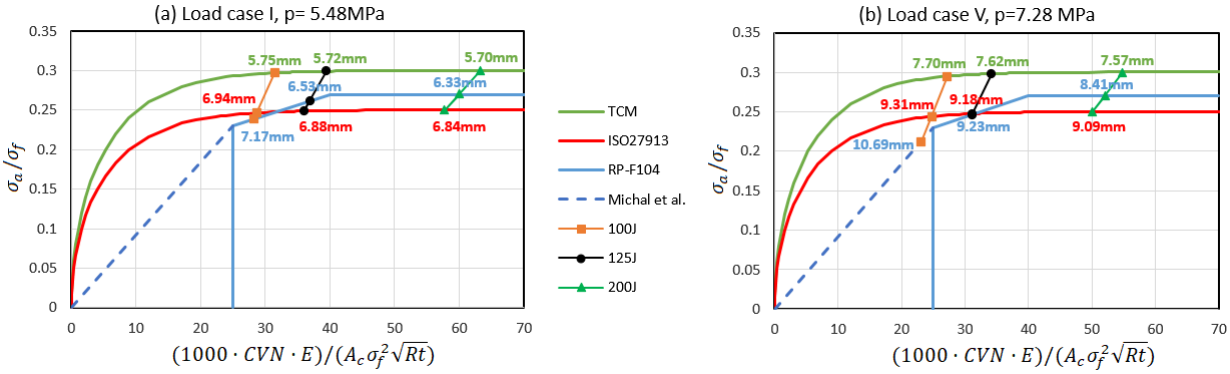

Figure 7 Minimum wall thickness for three different criteria for (a) load case I and (b) load case V

5. CONCLUSIONS

The proposed pipeline dimensions for the Northern Lights pipeline, which is an integral part of the full-scale CO_2 project Longship, have been assessed with respect to running-ductile fracture following the updated TCM methodology in DNVGL-RP-F104. The main conclusion is that, for the given pipe material and diameter, and the given loading conditions, a wall thickness of 15.9 mm is sufficient for arresting a propagating crack. The TCM with the new empirical criteria for the arrest/propagate boundary is shown to have better sensitivity with respect to the materials CVN value than the previous proposed criteria. Further, although the empirical data giving arrest is mainly from high-toughness pipes, the method is more conservative than the previous TCM approach for low toughness pipelines, but more research is needed to improve the method for low toughness or high strength pipes. In a future study, we plan to investigate numerically the low-toughness / high strength region for the Northern Lights pipeline.

5. ACKNOWLEDGEMENTS

The main author would like to acknowledge the support from the NCCS Research Centre, performed under the Norwegian research program Centres for Environment-friendly Energy Research (FME), supported by the Research Council of Norway (257579/E20).

6. REFERENCES

Andrews, R. M., Batte, A. D., Lowesmith, B. J. & Millwood, N. A. (2003). “THE FRACTURE ARREST BEHAVIOUR OF 914 MM DIAMETER X100 GRADE STEEL PIPELINES”. *Biennal Joint Technical Meeting on Pipeline Research.* Berlin.

Aursand, E., Dumoulin, S., Hammer, M., Lange, H. I., Morin, A., Munkejord, S. T. & Nordhagen, H. O. (2016). “Fracture propagation control in CO2 pipelines: Validation of a coupled fluid–structure model”. *Engineering Structures,* 123**,** 192-212.

Barnett, J. & Cooper, R. (2014). The COOLTRANS Research Programme: Learning for the Design of CO2 Pipelines. *ASME Paper No. IPC2014-33370.*

Burdekin, F. M. & Stone, D. E. W. (1966). “The crack opening displacement approach to fracture mechanics in yielding materials”. *Journal of Strain Analysis,* 1**,** 145-153.

Cosham, A. (2012). “The saturation pressure and the design of dense-phase carbon dioxide pipelines”. *3rd International forum on the transportation of CO2 by pipeline.*

Cosham, A., Jones, D. G., Armstrong, K., Allason, D. & Barnett, J. (2012). “Ruptures in Gas Pipelines, Liquid Pipelines and Dense Phase Carbon Dioxide Pipelines”. *ASME Paper No. IPC2012-90463*.

Cosham, A., Jones, D. G., Armstrong, K., Allason, D. & Barnett, J. (2014). “Analysis of two dense phase carbon dioxide full-scale fracture propagation tests”. *ASME Paper No. IPC2014-33080*.

Cosham, A., Jones, D. G., Armstrong, K., Allason, D. & Barnett, J. (2016). “Analysis of a Dense Phase Carbon Dioxide Full-Scale Fracture Propagation Test in 24 Inch Diameter Pipe”. *ASME Paper No. IPC2016-64456*.

Demofonti, G., Mannucci, G., Vito, L. D., Aristotile, R., Biagio, M., Malatesta, G., Harris, D. & Harrison, P. (2005). “Ultra-high-strength pipeline prototyping for natural gas transmission Demopipe”.

Di Biagio, M., Lucci, A., Mecozzi, E. & Spinelli, C. M. (2017). “Fracture Propagation Prevention on CO2 pipelines: Full Scale Experimental Testing and Verification Approach”. *Pipeline Technology Conference 2017.* Berlin.

DNV-GL (2017). “DNVGL-RP-F104 Design and operation of CO2 pipelines”.

DNV-GL (2021). “DNVGL-RP-F104 Design and operation of CO2 pipelines”.

Gruben, G., Dumoulin, S., Nordhagen, H., Hammer, M. & Munkejord, S. T. (2018a). “Simulation of a Full-Scale CO2 Fracture Propagation Test”. *ASME Paper No. IPC2018-78631*.

Gruben, G., Macdonald, K., Munkejord, S. T., Skarsvåg, H. L. & Dumoulin, S. (2020). Pipeline Fracture Control Concepts for Norwegian Offshore Carbon Capture and Storage. *ASME Paper No. IPC2020-9766*.

Gruben, G., Nyhus, B., Munkejord, S. T., Dumoulin, S., Nordhagen, H., Lange, H. & Skarsvåg, H. L. (2018b). “FCP Northern Lights”. SINTEF Report 2018:00425.

ISO/TC 265 (2016). “ISO 27913:2016 Carbon dioxide capture, transportation and geological storage -Pipeline transportation systems”.

Keim, V., Paredes, M., Nonn, A. & Münstermann, S. (2020). “FSI-simulation of ductile fracture propagation and arrest in pipelines: Comparison with existing data of full-scale burst tests”. *International Journal of Pressure Vessels and Piping,* 182**,** 104067.

Leis, B. N., Eiber, R. J., Carlson, L. & Gilroy-Scott, A. (1998) Relationship between apparent (total) Charpy vee-notch toughness and the corresponding dynamic crack-propagation resistance. *ASME Paper No. IPC1998-2084*.

Linton, V., Leinum, B. H., Newton, R. & Fyrileiv, O. (2018). “CO2SAFE-ARREST: A Full-Scale Burst Test Research Program for Carbon Dioxide Pipelines — Part 1: Project Overview and Outcomes of Test 1”. *ASME Paper No. IPC2018-78517*.

Mahgerefteh, H., Brown, S. & Denton, G. (2012). “Modelling the impact of stream impurities on ductile fractures in CO2 pipelines”. *Chemical Engineering Science*.

Maxey, W., Kiefner, J., Eiber, R. & Duffy, A. (1972). Ductile fracture initiation, propagation, and arrest in cylindrical vessels. *Fracture Toughness: Part II*. ASTM International.

Maxey, W. A. (1974). “Fracture Initiation, Propagation and Arrest”. *5th Symposium on Line Pipe Research.* Huston, TX

Maxey, W. A. (1986). “Long Shear Fractures in CO2 Lines Controlled by Regulating Saturation Arrest Pressures”. *Oil and Gas Journal,* 84**,** 44-46.

Michal, G., Østby, E., Davis, B., Røneid, S. & Lu, C. (2020). An Empirical Fracture Control Model for Dense-Phase CO2 Carrying Pipelines. *ASME Paper No. IPC2020-9421*.

Munkejord, S. T., Deng H., Austegard, A., Hammer, M., Aasen A. & Skarsvåg, H. L. (2021) “Depressurization of CO2-N2 and CO2-He in a pipe: Experiments and modelling of pressure and temperature dynamics”. *International Journal of Greenhouse Gas Control*, 109,

Nakai, H., Shibanuma, K. & Aihara, S. (2016). “Numerical model for unstable ductile crack propagation and arrest in pipelines using finite difference method”. *Engineering Fracture Mechanics,* 162**,** 179-192.

Nonn, A., Keim, V. & Münstermann, S. (2020). “Towards an Improved Prediction of Fracture Behavior in Pipelines Using the Coupled Fluid-Structure Interaction (FSI) Model”. *The 30th International Ocean and Polar Engineering Conference.* Virtual: International Society of Offshore and Polar Engineers.

O'Donoghue, P. E., Kanninen, M. F., Leung, C. P., Demofonti, G. & Venzi, S. (1997). “The development and validation of a dynamic fracture propagation model for gas transmission pipelines”. *International Journal of Pressure Vessels and Piping,* 70**,** 11-25.

Papka, S. D., Stevens, J. H., Macia, M. L., Fairchild, D. P. & Petersen, C. W. (2003). Full-size testing and analysis of X120 linepipe. 13th International Offshore and Polar Engineering Conference, Honolulu, Hi. International Society Offshore& Polar Engineers, 50-59.

Shim, D.-J., Wilkowski, G., Rudland, D., Rothwell, B. & Merritt, J. (2008). “Numerical Simulation of Dynamic Ductile Fracture Propagation Using Cohesive Zone Modeling”. *ASME Paper No. IPC2008-64049*.

Span, R. & Wagner, W. (1996). “A New Equation of State for Carbon Dioxide Covering the Fluid Region from the Triple-Point Temperature to 1100 K at Pressures up to 800 MPa”. *Journal of Physical and Chemical Reference Data,* 25**,** 1509-1596.

Wilkowski, G., Maxey, W. & Eiber, R. (1977). Use of a brittle notch DWTT specimen to predict fracture characteristics of line pipe steels. ASME 1977 Energy Technology Conference, Houston, TX, Paper, 1977. 18-22.